

Research Article

# Structural Performance Analysis of the Classroom Building at the South Minahasa Marine Training and Education Center Using the Pushover Method

Femmy The <sup>1\*</sup>, Steenie E. Wallah <sup>2</sup>, Marthin D. J. Sumayouw <sup>3</sup>

<sup>1</sup> Program Pascasarjana, Universitas Sam Ratulangi, Manado, Indonesia; email : [fentreyzathe07@gmail.com](mailto:fentreyzathe07@gmail.com)

<sup>2</sup> Program Pascasarjana, Universitas Sam Ratulangi, Manado, Indonesia; email : [wsteenie@yahoo.com](mailto:wsteenie@yahoo.com)

<sup>3</sup> Program Pascasarjana, Universitas Sam Ratulangi, Manado, Indonesia; email : [dody\\_sumajouw@unsrat.ac.id](mailto:dody_sumajouw@unsrat.ac.id)

\* Corresponding Author : Femmy The

**Abstract:** Minahasa Selatan is a region with high seismic activity, requiring accurate structural design and evaluation against earthquake loads. This study aims to evaluate the seismic performance of a classroom building at the Marine Training and Education Center in Minahasa Selatan using the pushover method within a performance-based seismic design approach. The main issue addressed is how different response spectra—SNI 1726:2019 and the Indonesian Design Spectrum—affect structural performance assessment. The methodology includes literature review, structural modeling based on Asbuilt Drawings, and pushover analysis using SAP2000 software, referencing FEMA-356, FEMA-440, and ATC-40 guidelines. Results indicate that the SNI 1726:2019 spectrum yields higher shear forces and displacements compared to the Indonesian Design Spectrum, though the difference remains below 3%. Maximum shear force reaches 19,716.449 kN and displacement is 0.173 m (FEMA-440), while ATC-40 yields a minimum displacement of 0.1456 m and base shear of 3985.007 kN. The analysis places the structure within the Life Safety (LS) to Collapse Prevention (CP) performance range, suggesting it can maintain global stability and protect occupants during seismic events despite reduced stiffness. The study concludes that the building remains structurally safe and functionally adequate after an earthquake, and that variations in the response spectra result in limited impact on performance evaluation outcomes.

**Keywords:** Earthquake; Pushover; Structural Performance; Response Spectrum; SAP2000.

## 1. Introduction

Multi-storey buildings are vertical structures composed of several floors, constructed as a solution to land limitations and increasing space demands [1], [2]. In Indonesia, the development of high-rise buildings continues to grow, including in areas with high seismic activity such as North Sulawesi. Geotechnically, Indonesia lies within a highly seismic region due to its location at the convergence of four major tectonic plates: the Eurasian, Indo-Australian, Pacific, and Philippine Plates [3], [4]. The interaction between these plates, combined with regional geological conditions, contributes to the frequency and intensity of earthquakes, particularly in South Minahasa. Data from BNPB (<https://gis.bnpb.go.id/>) indicates that this region has experienced several moderate to large earthquakes over the past decade, resulting in infrastructure damage, casualties, and tsunami threats. In such contexts, public facilities such as the South Minahasa Maritime Education and Training Center must be designed with adequate earthquake resistance.

In seismic-resistant structural design in Indonesia, the Indonesian National Standard (SNI) 1726 is commonly used, incorporating response spectrum analysis adjusted to local geotechnical and seismotectonic conditions [5]. However, recent advances in geospatial data and analytical technology have introduced an alternative: the Indonesian Design Spectrum, which employs Probabilistic Seismic Hazard Analysis (PSHA) for more detailed and up-to-date seismic modeling. One widely adopted method for structural performance evaluation is

Received: June 01, 2025

Revised: June 14, 2025

Accepted: June 28, 2025

Published: June 30, 2025

Curr. Ver.: June 30, 2025



Copyright: © 2025 by the authors.

Submitted for possible open

access publication under the

terms and conditions of the

Creative Commons Attribution

(CC BY SA) license

(<https://creativecommons.org/licenses/by-sa/4.0/>)

pushover analysis, a nonlinear static approach in which lateral seismic loads are incrementally applied to the mass center of each floor until the formation of plastic hinges. This method enables identification of critical structural components that contribute most to the nonlinear response under increasing seismic loads, providing insights into deformation capacities, stability, and detailing requirements.

This study aims to analyze the seismic performance of the classroom building at the South Minahasa Maritime Education and Training Center using the *pushover* method and compare the results based on response spectra from SNI 1726:2019 and the Indonesian Design Spectrum [5]. Structural modeling is based on *as-built* drawings and analyzed using SAP2000 version 20, referencing ATC-40, FEMA 356, and FEMA 440 guidelines. The analysis focuses on two horizontal directions (X and Y), considering only seismic lateral loads.

The scope of this research is limited to evaluating a five-story reinforced concrete building used for educational purposes, with the goal of assessing structural deformation capacity, seismic performance level, and post-earthquake serviceability. The findings are expected to contribute to better understanding of seismic performance in maritime educational facilities, offer practical references for performance-based building design, and support the development of local guidelines by comparing national and international design spectra standards.

## 2. Theoretical Studies

### 2.1. Seismic Design Approaches for Buildings

In recent decades, structural engineering has progressively adopted performance-based design approaches to better address seismic risks [6]. Traditional force-based design methods, while widely used, do not always capture the actual nonlinear behavior of structures under seismic loading. The concept of Performance-Based Seismic Design (PBSD) allows engineers to assess how structures perform under different levels of seismic intensity by setting performance objectives [7], [8], [9]. PBSD provides flexibility in selecting performance levels, from Immediate Occupancy (IO) to Life Safety (LS) and Collapse Prevention (CP), depending on building use and importance.

Seismic response spectrum is a key element in PBSD. It represents the maximum expected response of a structure to a particular ground motion and is used as a design input. SNI 1726:2019 outlines the seismic response spectra applicable in Indonesia, incorporating local seismicity, soil classification, and risk categories. Alternatively, the Indonesian Design Spectrum offers a more detailed approach, utilizing probabilistic seismic hazard analysis (PSHA) and actual earthquake data to generate region-specific spectra [10].

### 2.2. Pushover Analysis Methodology

Pushover analysis is a nonlinear static method employed to evaluate the seismic performance of building structures [11], [12]. The method incrementally applies lateral loads to a structural model until a target displacement is reached, revealing the capacity curve that maps base shear versus roof displacement. Pushover analysis is supported by several guidelines, notably ATC-40 for capacity spectrum method and FEMA-356/440 for displacement coefficient and modification methods. This analysis helps identify critical plastic hinge formations and their sequences, offering insight into potential failure mechanisms [13].

### 2.3. Prior Research and Research Gap

Several studies have demonstrated the usefulness of pushover analysis in assessing structural performance [14], [15]. Afif Salim applied the method to multi-story buildings in seismically active regions and confirmed its effectiveness in determining deformation capacity and performance level [16]. Dewobroto emphasized the need to consider different response spectra in nonlinear analysis, as spectrum choice significantly impacts displacement and base shear results [13]. However, most studies utilized only one type of response spectrum, either SNI or a general international standard.

This study addresses the gap by directly comparing the SNI 1726:2019 spectrum and the Indonesian Design Spectrum within the same structural analysis framework. By using the pushover method in SAP2000 and evaluating results using ATC-40, FEMA-356, and FEMA-440, the research provides a more comprehensive understanding of structural behavior under

different spectral inputs. This comparison is essential for improving the seismic resilience of educational facilities, especially in seismically active regions like South Minahasa.

### 3. Research Method

This research employed a quantitative approach through nonlinear static analysis using the pushover method. The object of the study was the five-story reinforced concrete classroom building of the South Minahasa Maritime Education and Training Center. Structural modeling was based on as-built drawings and implemented in the SAP2000 version 20 software. The building's structural system consists of a reinforced concrete moment-resisting frame. Lateral loads applied in the analysis were limited to earthquake loads, and the evaluation was conducted in two orthogonal directions: X and Y.

The seismic loads used in the analysis followed two different response spectra: those specified in SNI 1726:2019 and those derived from the Indonesian Design Spectrum. These spectra represent different methodologies—code-based versus site-specific probabilistic seismic hazard analysis—and were compared to evaluate their impact on performance results. The pushover analysis procedure referred to guidelines provided in ATC-40, FEMA 356, and FEMA 440 to assess structural performance levels such as Immediate Occupancy (IO), Life Safety (LS), and Collapse Prevention (CP).

The simulation involved gradually increasing lateral loads until the structure reached its target displacement [17], [18]. The resulting capacity curves were analyzed to determine base shear values, plastic hinge development, displacement performance, and critical failure zones. The comparison between different response spectra aimed to assess how spectrum selection influences the building's seismic performance classification. All results were synthesized to support recommendations for future earthquake-resistant design practices in educational buildings.

## 4. Result and Discussion

### 4.1 . Building Modeling and Seismic Load Configuration

The three-dimensional (3D) model of the Classroom Building at the Maritime Education and Training Center in South Minahasa was developed using SAP2000 software. The structural components, including beams, columns, and slabs, were modeled based on existing architectural and structural drawings. The model represents the complete spatial configuration of the building in the XY plane and vertical direction, as shown in Figure 1.

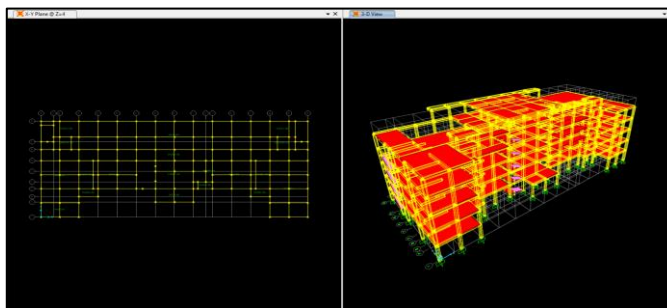


**Figure 1.** 3D and XY Direction Model of the Building

Seismic load analysis was conducted using the response spectrum method, referring to the Indonesian seismic code SNI 1726:2019 and the Indonesian Design Spectrum (IDS) provided by the national seismic hazard map (<https://rsa.ciptakarya.pu.go.id/2021/>). The site is classified as SC-type soil, corresponding to hard or dense soils and soft rock conditions.

The seismic parameters applied in the model are summarized in Table 1, derived from both the SNI 1726:2019 and the Indonesian Design Spectrum data for Amurang region.

**Table 1.** Seismic Parameters Used in the Model

Parameter	Value
Ss	1.5 g
S1	0.6 g
Fa	1.2
Fv	1.4
T1	20 s
I	1.5
R	8
$\Omega$	3
Cd	5.5

The seismic response spectrum curve for the Amurang region is presented in Figure 2, which was input into SAP2000 as the reference for dynamic response analysis. This spectrum serves as a basis for calculating internal forces, displacements, and structural demands under earthquake excitation.

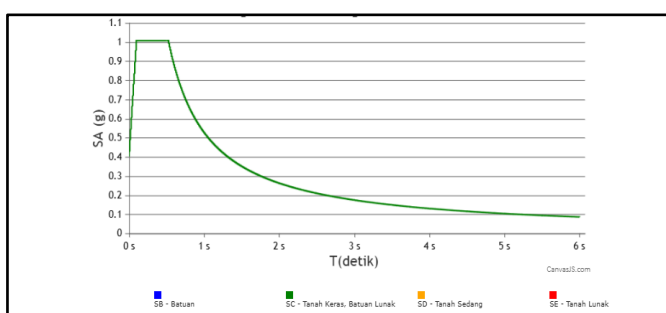


Figure 2. Seismic Response Spectrum for Amurang District (South Minahasa)

## 4.2 . Structural Validation: Modal Participation, Base Shear, and Inter-story Drift

### 4.2.1. Modal Participation Check

In accordance with SNI 1726:2019 Article 7.9.1.1, the total modal mass participation in dynamic analysis must reach at least 90% in each orthogonal horizontal direction (X and Y). This requirement ensures that the dynamic response of the structure is adequately represented through a sufficient number of vibration modes.

The SAP2000 analysis results confirmed that the cumulative mass participation exceeded 95% in both X and Y directions up to mode 12, satisfying the regulatory requirement. This is illustrated in Figure 3, which presents the modal mass participation ratio summaries for both spectra.

Output Case	Step Type	Step Number	Period Sec	UX	UY	UZ	SumUX	SumUY	SumUZ	RX
MODAL	Mode	1	0.786027	0.2	0.000223	0.294E-07	0.0	0.000223	0.294E-07	7.895E-01
MODAL	Mode	2	0.718958	0.0001369	0.668	2.058E-06	0.0	0.667	2.686E-06	0.003
MODAL	Mode	3	0.690482	0.003811	0.138	4.591E-06	0.803	0.805	7.277E-06	0.012
MODAL	Mode	4	0.275495	0.108	0.0006999	2.885E-07	0.911	0.806	7.578E-06	0.001217
MODAL	Mode	5	0.259535	0.0005037	0.104	3.567E-05	0.912	0.91	4.324E-05	0.217
MODAL	Mode	6	0.252828	0.0001831	0.007069	1.311E-05	0.912	0.917	5.636E-05	0.015
MODAL	Mode	7	0.18913	0.04	0.000211	5.017E-06	0.952	0.917	6.138E-05	0.0003427
MODAL	Mode	8	0.158296	0.003059	0.024	0.0001829	0.955	0.941	0.0001643	0.023
MODAL	Mode	9	0.151195	0.00211	0.017	3.344E-07	0.957	0.957	0.0001646	0.011
MODAL	Mode	10	0.121229	0.000246	0.001317	0.0000547	0.958	0.958	0.0000193	0.0000012
MODAL	Mode	11	0.120496	7.437E-06	4.178E-06	0.018	0.958	0.958	0.019	0.012
MODAL	Mode	12	0.11818	2.314E-05	1.913E-05	0.002094	0.958	0.958	0.021	0.0002348

(a)

OutputCase	StepType	StepNum	Period	UX	UY	UZ	SumUX	SumUY	SumUZ	RX	RY	RZ
Text	Text	Unitless	Sec	Unitless	Unitless	Unitless	Unitless	Unitless	Unitless	Unitless	Unitless	Unitless
MODAL	Mode	1	0.786027	0.8	0.000223	6.294E-07	0.8	0.000223	6.294E-07	7.886E-06		
MODAL	Mode	2	0.719058	0.001388	0.666	2.056E-06	0.8	0.667	2.686E-06	0.083		
MODAL	Mode	3	0.690402	0.003811	0.138	4.591E-06	0.803	0.605	7.277E-06	0.012		
MODAL	Mode	4	0.275495	0.108	0.000699	2.865E-07	0.911	0.806	7.578E-06	0.001217		
MODAL	Mode	5	0.259535	0.000607	0.104	3.967E-05	0.912	0.91	4.324E-05	0.217		
MODAL	Mode	6	0.235328	0.001821	0.007089	1.311E-05	0.912	0.917	5.836E-05	0.016		
MODAL	Mode	7	0.16913	0.04	0.000211	5.617E-06	0.952	0.917	6.138E-05	0.0003427		
MODAL	Mode	8	0.158296	0.003059	0.024	0.0001029	0.955	0.941	0.0001643	0.023		
MODAL	Mode	9	0.151195	0.00211	0.017	3.344E-07	0.957	0.957	0.0001648	0.011		
MODAL	Mode	10	0.121229	0.0002345	0.001317	0.0005547	0.958	0.958	0.0007193	0.003632		
MODAL	Mode	11	0.120498	7.437E-06	4.178E-06	0.018	0.958	0.958	0.019	0.012		
MODAL	Mode	12	0.11818	2.314E-05	1.913E-05	0.002094	0.958	0.958	0.021	0.0002348		

(b)

Figure 3. Modal Mass Participation Ratios

(a) SNI 1726:2019 | (b) Indonesian Design Spectrum

#### 4.2.2. Base Shear Validation

To validate the seismic base shear, the results from the dynamic (response spectrum) analysis were compared against those from the equivalent static method, as required in SNI 1726:2019 Article 7.9.1.4. The dynamic base shear (VD) must not be less than the static base shear (VS), i.e.,  $VD \geq VS$ .

The SAP2000 output, shown in Figure 4, illustrates the selection of earthquake load cases and the resulting base reactions.

OutputCase	CaseType	StepType	GlobalFX	GlobalFY	GlobalFZ	GlobalMX	GlobalMY	GlobalMZ
Text	Text	Text	Kgf	Kgf	Kgf	Kgf-m	Kgf-m	Kgf-m
EQX	LinStatic		-741393.38	-2.75E-09	6.909E-09	1.603E-07	-11554016.5	11924350.11
EQY	LinStatic		-2.21E-09	-810442.73	2.219E-10	12565209.81	-1.137E-07	-28433267.7
RSX	LinRespSpec	Max	616664.98	203013.32	1229.75	3018021.82	9099945.67	11109782.35
RSY	LinRespSpec	Max	185820.33	674204.01	3468.65	10032956.18	2740488.38	22068580.21

(a)

OutputCase	CaseType	StepType	GlobalFX	GlobalFY	GlobalFZ	GlobalMX	GlobalMY	GlobalMZ
Text	Text	Text	Kgf	Kgf	Kgf	Kgf-m	Kgf-m	Kgf-m
EQX	LinStatic		-703166.78	-2.627E-09	6.479E-09	1.517E-07	-10958285.8	11309524.8
EQY	LinStatic		-2.205E-09	-768655.91	3.52E-10	11917341.46	-1.13E-07	-26967234.6
RSX	LinRespSpec	Max	582945.4	194695.71	1062.85	2912223.99	8657296.25	10549320.06
RSY	LinRespSpec	Max	175638.96	646712.2	3016.53	9681367.83	2607251.82	21144959.34

(b)

Figure 4. Base Shear Output

(a) SNI 1726:2019 | (b) Indonesian Design Spectrum

In both spectrum scenarios, the computed base shear from the dynamic analysis met or exceeded the static base shear values, eliminating the need for scaling corrections.

#### 4.2.3. Inter-story Drift Check

The inter-story drift ratio was evaluated to ensure that the building's lateral deformation under seismic loading remained within acceptable serviceability limits. According to SNI 1726:2019, the maximum allowable drift ratio is 1.5% of story height.

Displacement data for selected joints were obtained using SAP2000. The difference in displacement between two adjacent floors ( $\Delta$ ) was computed and compared to the allowable value ( $\Delta_a = 0.015 \times h_{sx}$ ). The results, presented in Tables 2 and 3, show that all drift values in both X and Y directions are within permissible limits.

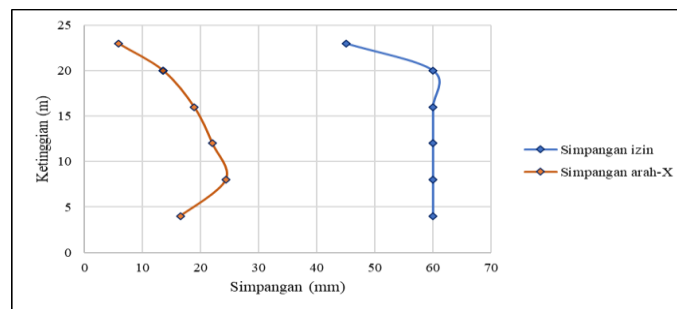
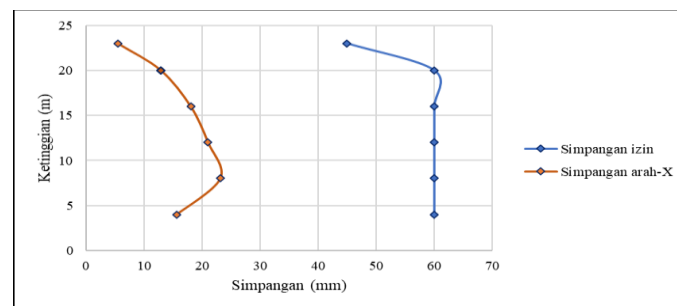
**Table 2.** Inter-story Drift in X-direction ( $\Delta x$ ) (SNI 1726:2019)

Floor	Joint	$h_{sx}$	$\square_x$	$\Delta a$ (Allowed)	$\Delta x$	Remark
		(mm)	(mm)	(mm)	(mm)	
Top Roof	932	3000	27,5827	45	5,7904	Safe
Roof	476	4000	26,0035	60	13,5722	Safe
4	475	4000	22,3020	60	18,8929	Safe
3	474	4000	17,1494	60	22,0242	Safe
2	473	4000	11,1428	60	24,3492	Safe
1	472	4000	4,5021	60	16,5077	Safe

**Table 3.** Inter-story Drift in Y-direction ( $\Delta y$ ) (SNI 1726:2019)

Floor	Joint	$h_{sy}$	$\square_y$	$\Delta a$ (Allowed)	$\Delta y$	Remark
		(mm)	(mm)	(mm)	(mm)	
Top Roof	932	3000	26,0616	45	7,5163	Safe
Roof	476	4000	24,0117	60	12,9774	Safe
4	475	4000	20,4724	60	17,6224	Safe
3	474	4000	15,6663	60	19,5826	Safe
2	473	4000	10,3256	60	21,8222	Safe
1	472	4000	4,3741	60	16,0384	Safe

Additionally, Figures 5 and 6 depict the drift distribution along the building height for both directions.

**Figure 5.** Inter-story Drift Diagram vs. Building Height (X-direction) (SNI 1726:2019)**Figure 6.** Inter-story Drift Diagram vs. Building Height (Y-direction) (SNI 1726:2019)

The same procedures were applied for the Indonesian Design Spectrum, as summarized in Tables 4 and 5, confirming that the structural drift remains well below the code limits.

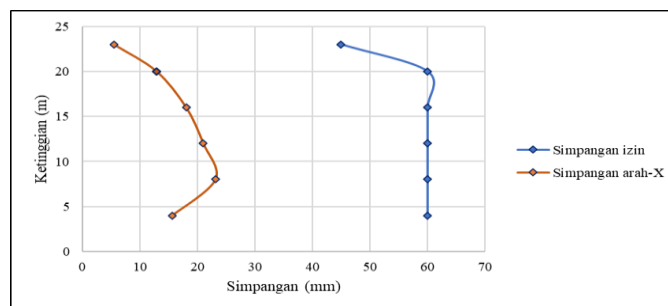
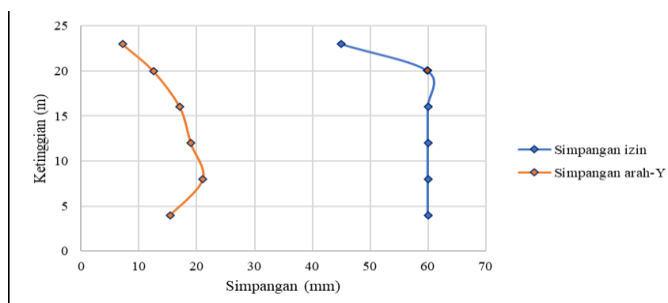
**Table 4.** Inter-story Drift in X-direction ( $\Delta x$ ) (Indonesian Design Spectrum)

Floor	Joint	$h_{sx}$	$\square_x$	$\Delta a$ (Allowed)	$\Delta x$	Remark
		(mm)	(mm)	(mm)	(mm)	
Top Roof	932	3000	26,2291	45	5,4589	Safe
Roof	476	4000	24,7403	60	12,8902	Safe

4	475	4000	21,2248	60	18,0312	Safe
3	474	4000	16,3072	60	21,0137	Safe
2	473	4000	10,5762	60	23,1455	Safe
1	472	4000	4,2638	60	15,6339	Safe

**Table 5.** Inter-story Drift in Y-direction ( $\Delta y$ ) (Indonesian Design Spectrum)

Floor	Joint	$h_{sx}$	$\square_y$	$\Delta a$ (Allowed)	$\Delta y$	Remark
		(mm)	(mm)	(mm)	(mm)	
Top Roof	932	3000	25,1288	45	7,1951	Safe
Roof	476	4000	23,1665	60	12,5041	Safe
4	475	4000	19,7563	60	17,0540	Safe
3	474	4000	15,1052	60	18,9464	Safe
2	473	4000	9,9380	60	21,0349	Safe
1	472	4000	4,2012	60	15,4044	Safe

**Figure 7.** Inter-story Drift Diagram vs. Building Height (X-direction) (Indonesian Design Spectrum)**Figure 8.** Inter-story Drift Diagram vs. Building Height (Y-direction) (Indonesian Design Spectrum)

The results indicate that the structure responds elastically under both spectrum inputs, and the overall lateral displacements are acceptable for occupancy and safety under seismic design loads.

#### 4.3 . Nonlinear Pushover Performance

To evaluate the nonlinear behavior of the structure under lateral seismic loading, a push-over analysis was performed using SAP2000. The analysis followed a two-stage loading process:

- Gravity loading, consisting of dead and live loads, was first applied under nonlinear static conditions.
- Subsequently, lateral loads were applied in the X and Y directions, with the initial condition set as the final state from the gravity load stage using the "Continue from State at End of Nonlinear Case" option.

Figures 9 and 10 illustrate the SAP2000 input configuration for the gravity and lateral loads.



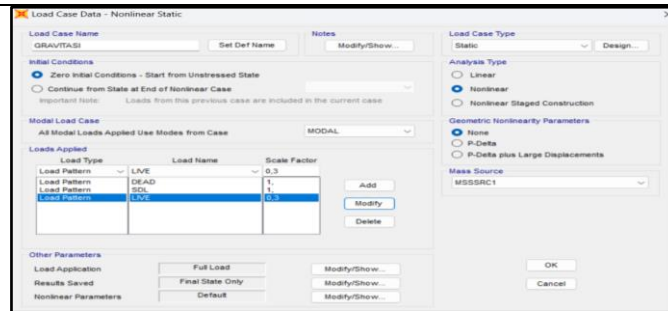


Figure 9. Gravity Load Dialog Box

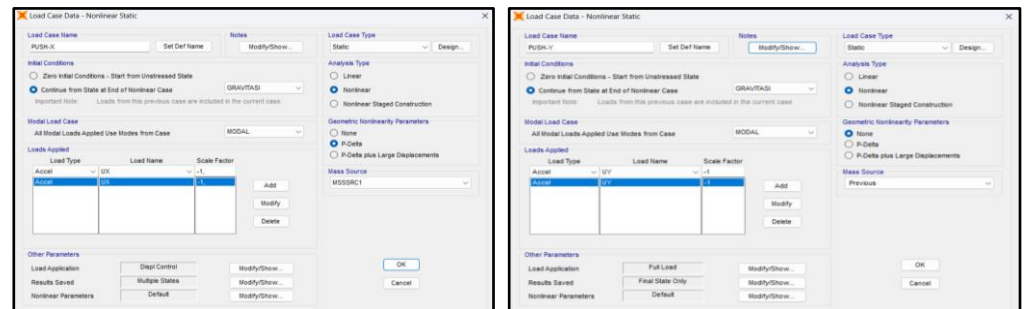


Figure 10. Lateral Load Input (X and Y Directions)

The resulting pushover analyses produced capacity curves that depict the relationship between base shear and lateral displacement. These curves were used to examine the structure's strength and deformation characteristics during seismic loading.

#### 4.3.1. Capacity Curves Based on SNI 1726:2019

The capacity curves generated using the FEMA 356 coefficient method with SNI 1726:2019 are shown in:

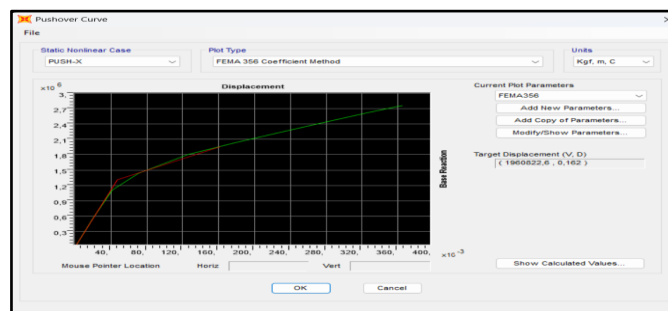


Figure 11. Building Capacity Curve due to Pushover in X-Direction (FEMA 356, SNI 1726:2019)

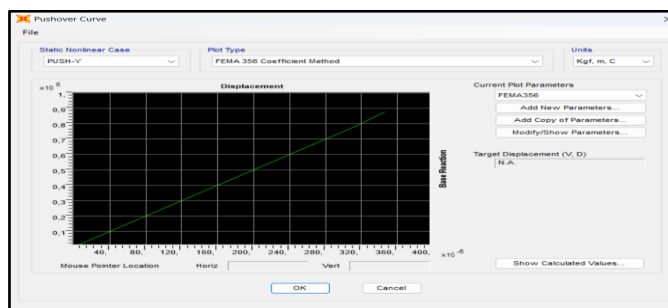


Figure 12. Building Capacity Curve due to Pushover in Y-Direction (FEMA 356, SNI 1726:2019)

The X-direction curve reached a maximum displacement of 0.36437 m and base shear of 265.02 kN at Step 14 (Table 6). In contrast, the Y-direction analysis terminated at Step 2, with a displacement of 0.000346 m and base shear of 84.35 kN (Table 7).



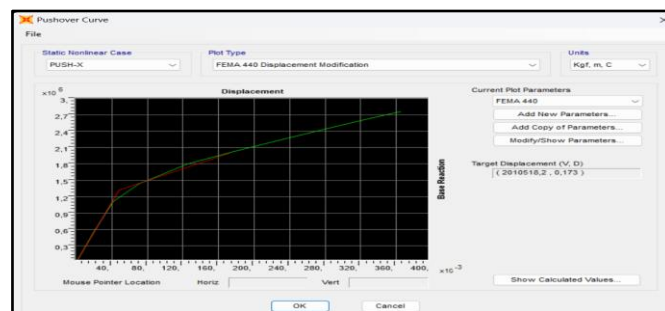
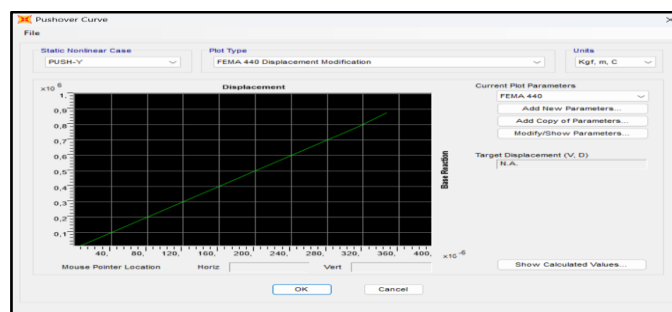
**Table 6.** Display Table of Pushover Curve in X-Direction (FEMA 356, SNI 1726:2019)

Load Case	Step	Displacement (m)	Base Force (kN)
Push-X	0	0	0
Push-X	1	0.020207	55.288
Push-X	2	0.040762	106.806
Push-X	3	0.070274	137.804
Push-X	4	0.070274	137.804
Push-X	5	0.070279	137.816
Push-X	6	0.125748	173.325
Push-X	7	0.178806	195.581
Push-X	8	0.228849	215.387
Push-X	9	0.279296	234.361
Push-X	10	0.326729	252.185
Push-X	11	0.361225	263.979
Push-X	12	0.361405	263.989
Push-X	13	0.364280	265.024
Push-X	14	0.364370	265.019

**Table 7.** Display Table of Pushover Curve in Y-Direction (FEMA 356, SNI 1726:2019)

Load Case	Step	Displacement (m)	Base Force (kN)
Push-Y	0	0	0
Push-Y	1	0.000315	75.677
Push-Y	2	0.000346	84.347

The same analysis using FEMA 440 yielded similar capacity curves, shown in Figures 13 and 14, and corresponding tabular data in Tables 6 and 7 (same data).

**Figure 13.** Building Capacity Curve due to Pushover in X-Direction (FEMA 440, SNI 1726:2019)**Figure 14.** Display Table of Pushover Curve in Y-Direction (FEMA 440, SNI 1726:2019)

#### 4.3.2. Capacity Curves Based on Indonesian Design Spectrum

For the Indonesian Design Spectrum, capacity curves using FEMA 356 are shown in:

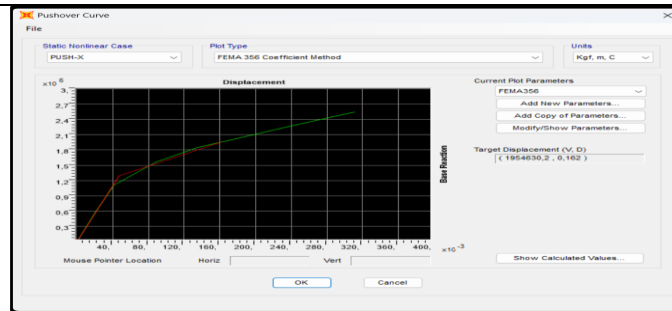


**Figure 15.** Building Capacity Curve due to Pushover in X-Direction (FEMA 356, Indonesian Design Spectrum)

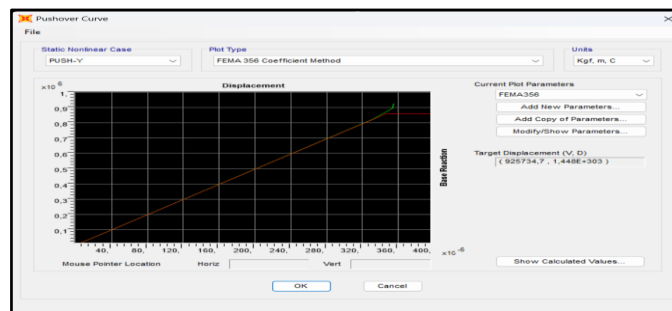


**Figure 16.** Building Capacity Curve due to Pushover in Y-Direction (FEMA 356, Indonesian Design Spectrum)

The X-direction pushover stopped at Step 8, with a displacement of 0.310809 m and base shear of 244.98 kN (Table 8). The Y-direction stopped at Step 6, with 0.000355 m displacement and 89.03 kN base shear (Table 9).

**Table 8.** Display Table of Pushover Curve in X-Direction (FEMA 356, Indonesian Design Spectrum)

Load Case	Step	Displacement (m)	Base Force (kN)
Push-X	0	0	0
Push-X	1	0.020207	55.288
Push-X	2	0.040781	106.816
Push-X	3	0.087908	150.654
Push-X	4	0.135344	177.671
Push-X	5	0.186106	197.479
Push-X	6	0.233544	216.195
Push-X	7	0.284934	235.586
Push-X	8	0.310809	244.977

**Table 9.** Display Table of Pushover Curve in Y-Direction (FEMA 356, Indonesian Design Spectrum)

Load Case	Step	Displacement (m)	Base Force (kN)
Push-Y	0	0	0
Push-Y	1	0.000332	79.416
Push-Y	2	0.000353	85.930
Push-Y	3	0.000354	86.495
Push-Y	4	0.000354	87.295
Push-Y	5	0.000354	87.473
Push-Y	6	0.000355	89.028

Analysis with FEMA 440 under the same spectrum also produced comparable results, as presented in Figures 17 and 18, and detailed in Tables 8 and 9 (same data).

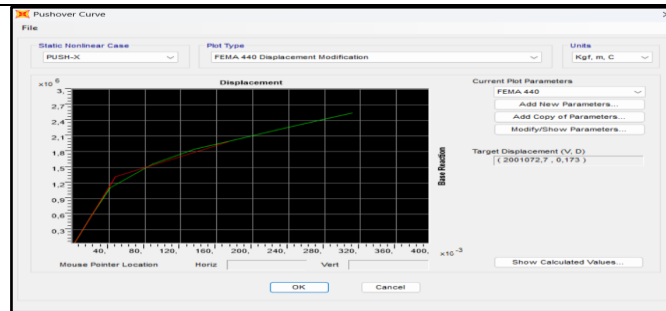


**Figure 17.** Building Capacity Curve due to Pushover in X-Direction (FEMA 440, Indonesian Design Spectrum)

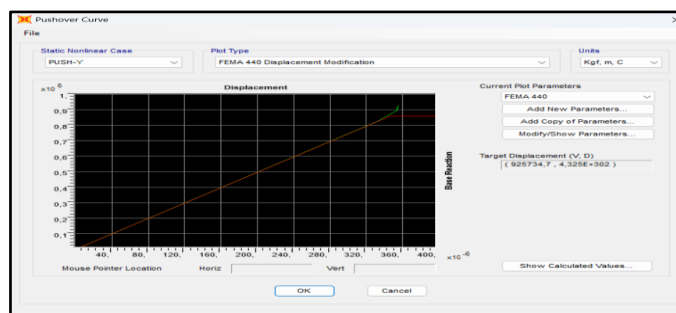


**Figure 18.** Building Capacity Curve due to Pushover in Y-Direction (FEMA 356, Indonesian Design Spectrum)

These capacity curves confirm that the structure demonstrates elastic-plastic behavior under increasing lateral loads. The X-direction exhibits a larger deformation and base shear capacity compared to the Y-direction, likely due to its longer moment frame configuration. These findings form the basis for evaluating the building's displacement targets and seismic performance levels, which are discussed in the next section.

#### 4.4 . Structural Performance Evaluation

To determine the structural performance level under seismic loading, target displacements were calculated using three established methods: FEMA 356, FEMA 440, and ATC-40 [19]. The performance point obtained from each method was used to classify the expected structural behavior in both X and Y directions.

##### 4.4.1. Target Displacement Results

The displacement targets for each method were determined based on the intersection between the capacity curve and the demand spectrum. These performance points reflect the maximum expected response during a design-level earthquake and are summarized in Table 10 (X direction) and Table 11 (Y direction).

**Table 10.** Comparison of Target Displacement and Base Shear – X Direction

Method	Target Displacement (m)		Base Shear Force (kN)	
	SNI 1726:2019	Indonesian Design Spectrum	SNI 1726:2019	Indonesian Design Spectrum
FEMA 356	0,162	0,162	19229,101	19168,374
FEMA 440	0,173	0,173	19716,449	19623,82
ATC 40	0,013	0,012	3731,275	4788,427

From the X-direction analysis:

- FEMA 440 with SNI 1726:2019 yielded the highest target displacement, at 0.173 m, with a base shear of 19,716.45 kN.
- ATC-40 provided the lowest displacement, 0.013 m, with base shear 3,731.28 kN.
- Both FEMA 356 and 440 suggest the structure achieves Life Safety (LS) performance, indicating the building maintains global stability and occupant safety with tolerable structural damage.

**Table 11.** Comparison of Target Displacement and Base Shear – Y Direction

Method	Target Displacement (m)		Base Shear Force (kN)	
	SNI 1726:2019	Indonesian Design Spectrum	SNI 1726:2019	Indonesian Design Spectrum
<i>FEMA 356</i>	0,162	0,162	19229,101	9078,356
<i>FEMA 440</i>	0,173	0,173	19716,449	9078,356
<i>ATC 40</i>	0,1499	0,1456	4080,425	3985,007

In the Y direction:

- The FEMA 440 method again produced the highest displacement (0.173 m), while ATC-40 resulted in the lowest (0.1456 m).
- FEMA-based analyses consistently classify the Y-direction response as Life Safety (LS), confirming the structure's capacity to remain functional and safe under seismic stress [20].

#### 4.4.2. Evaluation Summary

Overall, the results indicate that the Classroom Building at the Maritime Education and Training Center achieves a Life Safety (LS) performance level in both principal directions. The structure:

- Withstands design-level earthquakes without collapse,
- Maintains global stability,
- Preserves the safety of occupants, and
- Retains some reserve strength for post-earthquake occupancy.

These findings support the conclusion that the building complies with the performance-based design objectives outlined in FEMA and ATC guidelines.

#### 4.5 . Plastic Hinge Development and Collapse Mechanism

To gain insight into the structural collapse mechanism, the distribution and progression of plastic hinges were examined at various analysis steps in both X and Y directions. The visualizations were extracted from representative external portal frames modeled in SAP2000 and illustrate the spread of nonlinear plastic behavior under increasing lateral loads.

Plastic hinge formation was classified based on performance levels (e.g., A-B, B-IO, IO-LS, LS-CP, and C-D), with color-coded indicators representing the degree of plasticity and damage severity, from initial yielding to incipient collapse.

##### 4.5.1. Plastic Hinge Formation – X Direction

- Step 1 – Initial Plastic Hinge Formation  
Plastic hinges first appeared at Step 1 of the Push-X analysis:
  - Lateral displacement: 0.020207 m
  - Base shear: 574,895.67 kg
- This is visualized in:

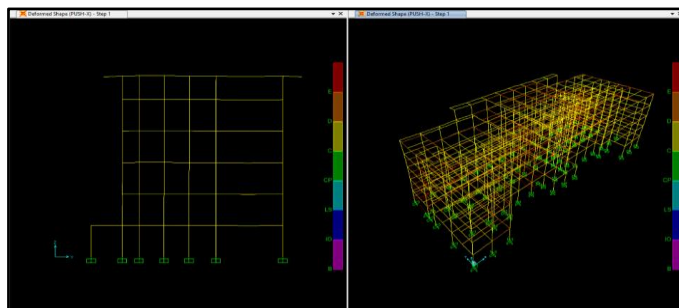


**Figure 19.** Distribution of Plastic Hinges on X-Direction Frame Step-1 due to Push X (SNI 1726:2019)

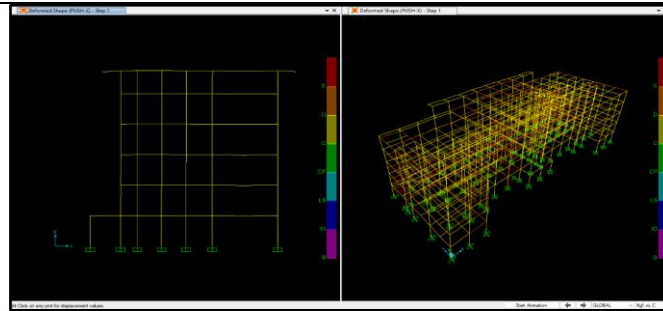


**Figure 20.** Distribution of Plastic Hinges on X-Direction Frame Step-1 due to Push X (Indonesian Design Spectrum)

Similarly, early hinge formation from Push-Y occurred at:

- Displacement: 0.000332 m
  - Base shear: 825,788.97 kg
- Shown in:

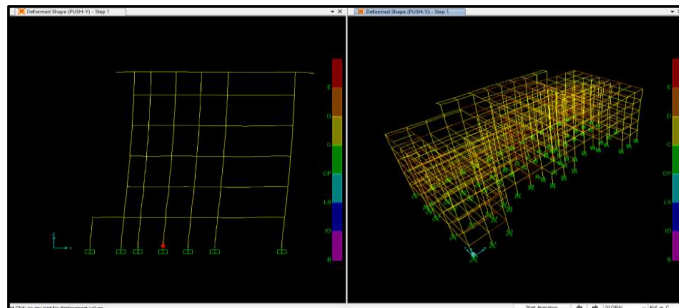


**Figure 21.** Distribution of Plastic Hinges on X-Direction Frame Step-1 due to Push Y (SNI 1726:2019)

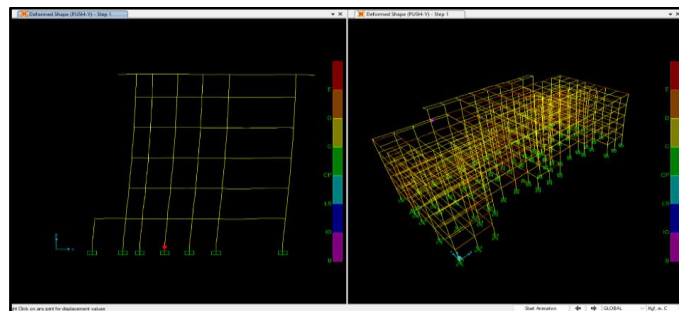


**Figure 22.** Distribution of Plastic Hinges on X-Direction Frame Step-1 due to Push Y (Indonesian Design Spectrum)

- Maximum Plastic Hinge Development  
At advanced steps, significant hinge development was observed:
  - Step 9 (Push-X, SNI): Displacement 0.381233 m, base shear 2,830,849.37 kg
  - Step 8 (Push-X, IDS): Displacement 0.310809 m, base shear 2,547,326.35 kg
- Visualized in:

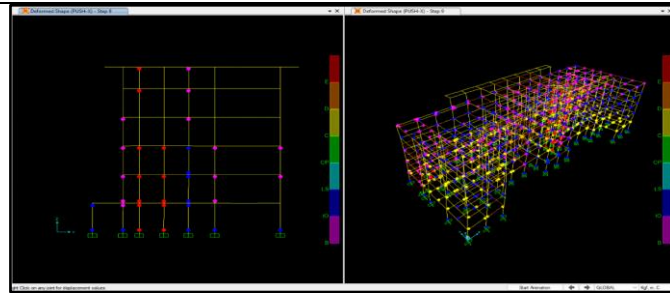


**Figure 23.** Distribution of Plastic Hinges on X-Direction Frame Step-9 due to Push X (SNI 1726:2019)

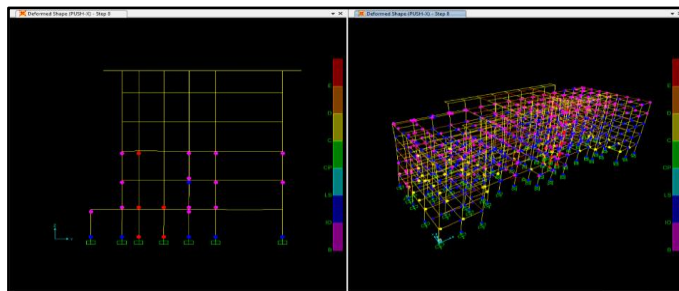


**Figure 24.** Distribution of Plastic Hinges on X-Direction Frame Step-8 due to Push X (Indonesian Design Spectrum)

These results indicate the appearance of Level B-IO hinges (Immediate Occupancy), signifying minimal structural damage and retained lateral stiffness. No components exceeded collapse thresholds.

Additional hinge development under Push-Y:

- Step 5 (SNI): Displacement 0.000295 m, base shear 1,314,750.2 kg
- Step 7 (IDS): Displacement 0.000352 m, base shear 957,996.26 kg

Visualized in:

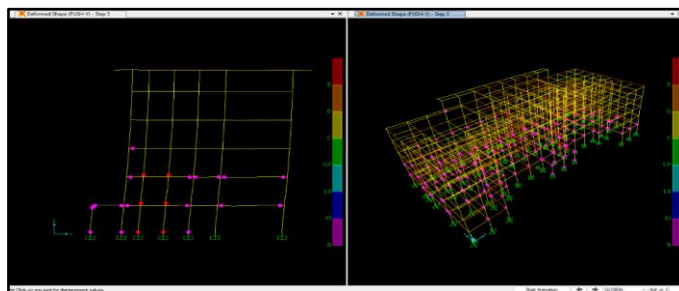


**Figure 25.** Distribution of Plastic Hinges on X-Direction Frame Step-5 due to Push Y (SNI 1726:2019)

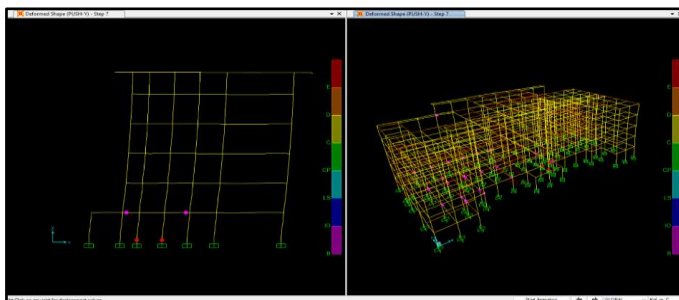


**Figure 26.** Distribution of Plastic Hinges on X-Direction Frame Step-7 due to Push Y (Indonesian Design Spectrum)

At this stage, hinges remained within the A-B range, meaning elastic behavior predominated.

#### 4.5.2. Plastic Hinge Formation – Y Direction

Patterns in the Y direction followed similar trends.

Initial hinge formation under Push-X:

- Step 1 displacement: 0.020207 m, base shear: 574,895.67 kg

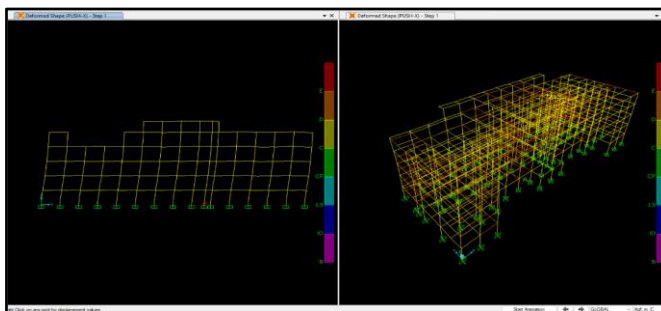


**Figure 27.** Distribution of Plastic Hinges on Y-Direction Frame Step-1 due to Push X (SNI 1726:2019)

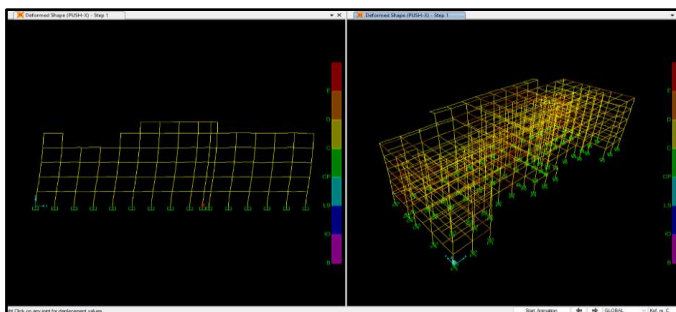


**Figure 28.** Distribution of Plastic Hinges on Y-Direction Frame Step-1 due to Push X (Indonesian Design Spectrum)

Under Push-Y:

- Displacement: 0.000332 m, base shear: 825,788.97 kg

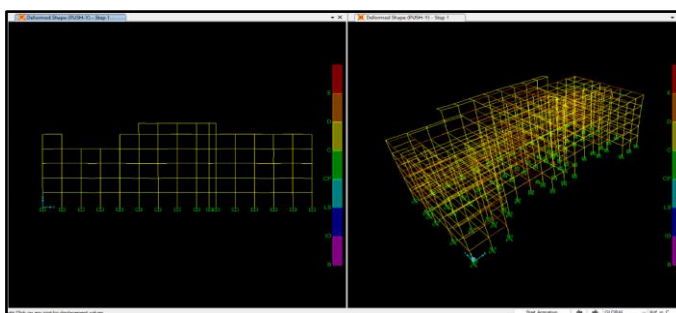


**Figure 29.** Distribution of Plastic Hinges on Y-Direction Frame Step-1 due to Push Y (SNI 1726:2019)

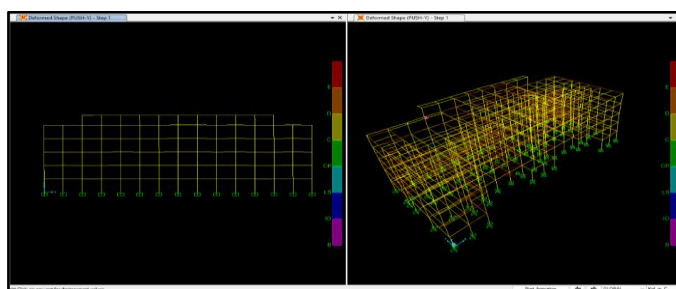




**Figure 30.** Distribution of Plastic Hinges on Y-Direction Frame Step-1 due to Push Y (Indonesian Design Spectrum)

Final significant hinge formation:

- Step 9 (Push-X, SNI): Displacement 0.381233 m, base shear 2,830,849.37 kg

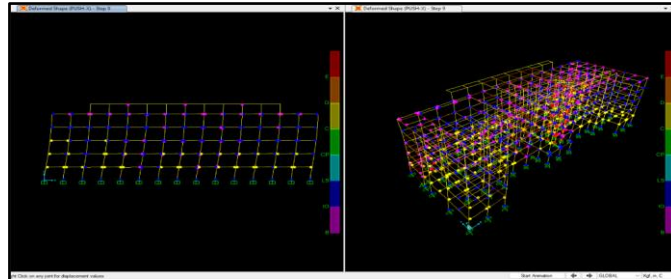


**Figure 31.** Distribution of Plastic Hinges on Y-Direction Frame Step-9 due to Push X (SNI 1726:2019)

- Step 8 (Push-X, IDS): Displacement 0.310809 m, base shear 2,547,326.35 kg

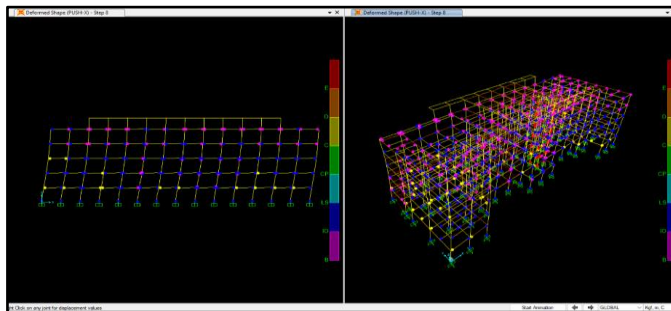


**Figure 32.** Distribution of Plastic Hinges on Y-Direction Frame Step-8 due to Push X (Indonesian Design Spectrum)

Push-Y analysis showed moderate hinge development:

- Step 5 (SNI): 0.000295 m, base shear: 1,314,750.2 kg
- Step 7 (IDS): 0.000352 m, base shear: 957,996.26 kg

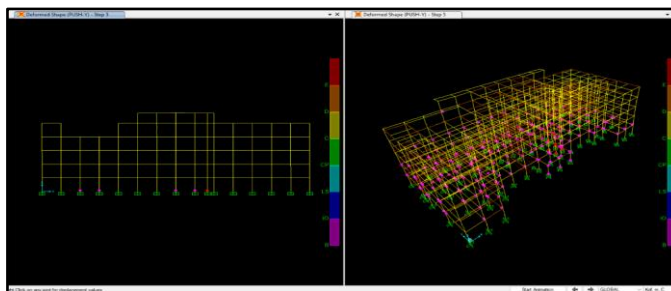


**Figure 33.** Distribution of Plastic Hinges on Y-Direction Frame Step-5 due to Push Y (SNI 1726:2019)

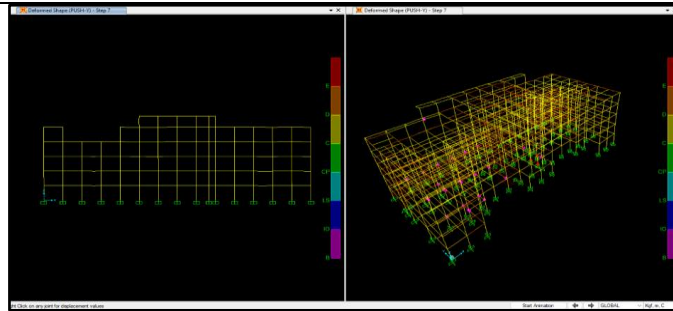


**Figure 34.** Distribution of Plastic Hinges on Y-Direction Frame Step-7 due to Push Y (Indonesian Design Spectrum)

Throughout all analyses, no plastic hinges exceeded LS-CP limits, and the plastic behavior remained controlled. The structural components showed no evidence of instability or progressive collapse, confirming that the building maintains adequate ductility and deformation capacity under seismic loading.

## 5. Conclusion

This study has evaluated the structural performance of the Classroom Building of the Maritime Training and Education Center in South Minahasa using pushover analysis based on the SNI 1726:2019 response spectrum and the Indonesian Design Spectrum. The results show that the building's performance falls within the range between Life Safety (LS) and Collapse Prevention (CP). This indicates that the structure has surpassed the LS threshold but has not yet entered a total collapse state. While the structure can still protect the lives of its occupants, it requires technical attention due to entering the damage zone, making it a basis for redesign and structural strengthening.

Furthermore, the SNI 1726:2019 response spectrum yields higher base shear forces than the Indonesian Design Spectrum. However, both spectra produce similar performance levels in the X direction (LS–CP), while in the Y direction, the building achieves Immediate Occupancy (IO), meaning it can remain fully operational after an earthquake, with only minor non-structural damage and minimal or no repair needed. The comparison between the two spectra reveals that differences in spectral parameters significantly affect performance evaluation. The Indonesian Design Spectrum shows higher acceleration values at short periods, increasing target displacements by approximately 3% based on ATC-40. According to FEMA 356, the structure generally achieves IO or LS performance under SNI 1726:2019, while under the Indonesian Design Spectrum, certain critical elements shift toward LS–CP, indicating reduced energy dissipation and increased plastic deformation. These findings highlight that the choice of response spectrum critically influences performance outcomes. Therefore, SNI 1726:2019 is more recommended for structural evaluation and design due to its more conservative acceleration and displacement parameters. Relying solely on the Indonesian Design Spectrum may lead to overestimating the building's performance and overlooking potential retrofitting needs.

To enhance future assessments and improve structural resilience, several recommendations are proposed. Further evaluation should be conducted on specific structural elements where plastic hinge concentrations are observed, particularly at beam supports and beam-column joints, to prevent excessive localized damage. The selection of structural materials and cross-sectional dimensions should be optimized to increase lateral load capacity and reduce the potential for early failure. Additionally, the use of nonlinear dynamic analysis methods such as time history analysis is encouraged to obtain a more accurate understanding of structural response under real earthquake conditions. Pushover analysis can also be complemented using other software tools like Perform3D, ETABS, or equivalent platforms for cross-validation. For future building designs located in high seismic risk zones, incorporating the Indonesian Design Spectrum as a supplementary reference—alongside SNI 1726:2019—can provide a broader safety margin and ensure more robust structural performance against various seismic scenarios.

**Author Contributions:** The author contributed fully to every stage of this research. Conceptualization: Femmy The; Methodology: Femmy The; Data Collection: Femmy The;

Data Validation and Analysis: Femmy The; Initial Draft Writing: Femmy The; Review and Editing: Femmy The; Supervision: [Ir. Steenie E. Wallah, M.Sc., Ph.D., IPU., Prof. Dr. Ir. M. D. J. Sumayouw, M.Eng, Ph.D].

**Funding:** This research did not receive any external funding. All expenses related to data collection, data processing, and report preparation were entirely borne by the author.

**Data Availability Statement:** The data supporting the findings of this study are available upon reasonable request from the corresponding author. The data include structural modeling files, pushover analysis results, as well as structural capacity and performance curves. However, as the data originate from an actual design project involving a government-owned educational institution, its distribution is restricted due to privacy considerations and institutional permissions. Therefore, the data cannot be publicly archived. Data requests will be considered in accordance with the policies and approval of the Balai Pendidikan dan Pelatihan Pelayaran Minahasa Selatan.

**Acknowledgments:** The author expresses sincere gratitude to the academic advisors [Ir. Steenie E. Wallah, M.Sc., Ph.D., IPU., and Prof. Dr. Ir. M. D. J. Sumayouw, M.Eng, Ph.D] for their guidance and direction during the preparation of this thesis. Appreciation is also extended to the management of the Balai Pendidikan dan Pelatihan Pelayaran Minahasa Selatan and PT. Pilar Dasar Membangun for providing the opportunity and permission to use data and structural information of the building as the subject of this study.

**Conflict of Interest:** The author declares no conflict of interest in the preparation and execution of this research. All analyses and interpretations were conducted objectively without external influence.

## References

- [1] M. Boen, "Mitigasi Risiko Gempa di Indonesia: Tantangan dan Strategi," *J. Tek. Sipil*, vol. 12, no. 2, pp. 105–116, 2011.
- [2] B. Suhardjono, "Perkembangan Bangunan Tinggi dan Tantangan Strukturalnya di Indonesia," in *Prosiding Seminar Nasional Teknik Sipil*, 2015, pp. 25–30.
- [3] D. P. Subagio and R. K. Nugroho, "Seismic Hazard Analysis for Indonesia Using Recent Plate Data," *J. Tek. Geofis.*, vol. 4, no. 1, pp. 21–30, 2016.
- [4] I. Meilano and others, "GPS Analysis of Crustal Deformation in Indonesia: Tectonic Implications," *J. Geophys. Res.*, vol. 114, no. B1, 2009.
- [5] SNI 1726:2019, *Tata Cara Perencanaan Ketahanan Gempa untuk Struktur Bangunan Gedung dan Non Gedung*. 2019.
- [6] S. Mazzoni, F. McKenna, M. H. Scott, and G. L. Fenves, "OpenSees Command Language Manual," 2006.
- [7] ATC-40, "Seismic Evaluation and Retrofit of Concrete Buildings," Redwood City, CA, 1996.
- [8] FEMA 440, "Improvement of Nonlinear Static Seismic Analysis Procedures," 2004.
- [9] FEMA 356, "Prestandard and Commentary for The Seismic Rehabilitation of Buildings," Nov. 2000.
- [10] K. PUPR, "SNI 1726:2019 – Tata Cara Perencanaan Ketahanan Gempa untuk Struktur Bangunan Gedung dan Non-Gedung," 2019.
- [11] D. P. Billah and A. Alam, "Seismic Performance of Concrete Frame Buildings Using Pushover Analysis," *Earthq. Spectra*, vol. 26, no. 3, pp. 803–818, 2010.
- [12] K. Chopra and R. Goel, "A Modal Pushover Analysis Procedure for Estimating Seismic Demands for Buildings," *Earthq. Eng. Struct. Dyn.*, vol. 31, pp. 561–582, 2002.
- [13] W. Dewobroto, "Evaluasi Kinerja Bangunan Baja Tahan Gempa dengan SAP2000," *J. Tek. Sipil*, vol. 3, no. 1, pp. 8–10, 2005.
- [14] N. Prihatmoko and others, "Analisis Perbandingan Pushover dan Analisis Dinamik Nonlinear," *J. Konstr.*, vol. 13, no. 2, pp. 117–123, 2019.
- [15] R. D. Tarigan and A. Sari, "Evaluasi Kinerja Struktur Bangunan Eksisting Menggunakan Metode Pushover," *J. Rekayasa Sipil*, vol. 15, no. 1, pp. 55–62, 2021.
- [16] A. B. S. Afif Salim, *Rekayasa Gempa*. Kepel Press, 2018.
- [17] T. Paulay and M. J. N. Priestley, *Seismic Design of Reinforced Concrete and Masonry Buildings*. Wiley, 1992.
- [18] H. Krawinkler and G. P. Reinhorn, "Pushover Procedure for Seismic Analysis," *J. Struct. Eng.*, vol. 123, no. 4, pp. 452–460, 1997.
- [19] H. Aschheim and M. Moehle, "Performance-Based Seismic Design Using Inelastic Response History Analysis," *Earthq. Spectra*, vol. 8, no. 3, pp. 439–461, 1992.
- [20] J. Moehle, "Displacement-Based Design of RC Structures Subjected to Earthquakes," *Earthq. Spectra*, vol. 18, no. 3, pp. 533–552, 2002.